# 4. Determination of the QPS Coil Set

The low aspect ratio (A = 2.6) and compact size of the two field-period QPS reference configuration, together with strong three-dimensional shaping and helical variation of the magnetic axis, present unique challenges for magnetic coil design. The coil system must be capable of preserving the physics capabilities of a reference plasma configuration while satisfying critical engineering design constraints. Favorable physics design characteristics are maintained through the accurate approximation of the magnetic field at the plasma boundary. Engineering constraints on coil current density and coil complexity are met through a combination of optimization targets aimed at increasing the minimum values of coil-coil separation, coil-plasma separation, and coil radius-of-curvature. In addition to these physics and engineering criteria, project cost considerations have led to rigid spatial constraints in the coil optimization model imposed by: (1) a maximum radial extent for modular coils in order to use an existing vacuum vessel, (2) the need for adequate access in the center of the torus for the center legs of the toroidal field (TF) and ohmic-current (OH) solenoid, and (3) the availability of existing vertical field (VF) ring coils from ATF.

## 4.1. Approach used to determine the reference coil set.

Methods have been developed to design practical modular coils for NCSX and QPS that achieve the desired physics properties while satisfying realistic engineering criteria necessary for their manufacture, construction, and access requirements. The approach used to optimize the modular coil set for the reference QPS configuration is illustrated in Figure 4.1.

A coil configuration consisting of modular, TF, OH, and VF coils has been selected for the reference QPS design. The method for determining the modular coil set is a generalization of a "reverse-engineering" [1] concept, which effectively separates the process of plasma optimization from that of coil design. The plasma optimization was performed with the STELLOPT code [2], while the coils were designed using the COILOPT code described in Appendix A. The reference plasma configuration was found through an extensive search of QPS parameter space by varying the plasma shape in a Levenberg-Marquardt optimization loop which uses a sequence of fixed-boundary VMEC [3] equilibrium solutions to target various equilibrium, stability and transport properties of the plasma. At low aspect ratios, it has been found to be useful (even imperative) to restrict the extensive search parameter space by including some figures-of-merit related to coil design in the plasma optimization step. This allows us to find a plasma configuration with a boundary shape and normal magnetic field distribution that can be reconstructed with a relatively small number of modular coils of moderate complexity ("kinkiness"). This ultimately results in a trade-off between plasma performance and project cost, and has been included in the QPS physics optimization analysis in the form of current density and complexity targets based on NESCOIL [4]. NESCOIL uses a surface-current to provide the external magnetic fields that determine a given plasma boundary. These NESCOIL solutions are easy to evaluate and therefore do not adversely impact the computational

performance of the rest of the physics optimization. The simultaneous determination of both a plasma boundary and filamentary coils is a computationally daunting task. Noteworthy is the observation that configurations with reduced current densities and complexity at the sheet current level also reflect similar improvements at the discrete modular coil level.

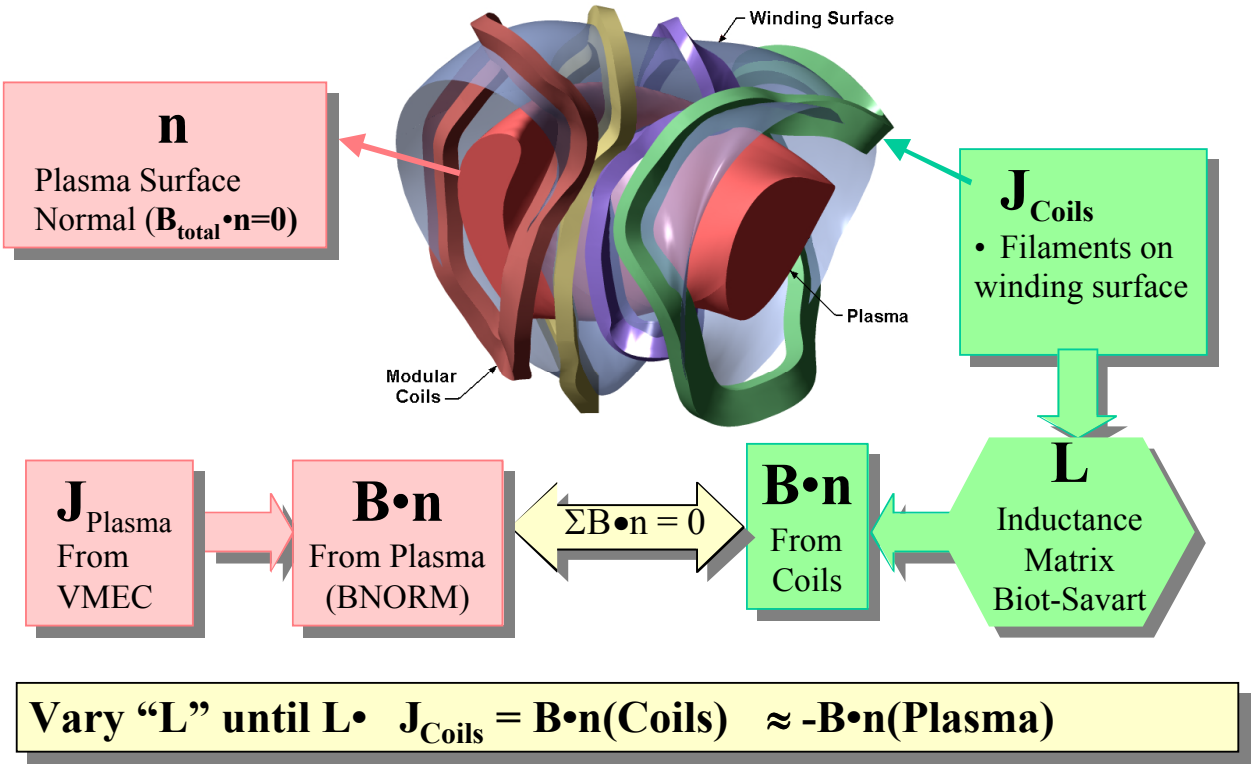


Figure 4.1. Procedure used to determine the optimum coil set to create the QPS plasma.

Filamentary modular coils are arranged on a coil winding surface (CWS) that initially approximately conforms to the reference plasma boundary, with adequate separation to allow space for the plasma scrape-off region, plasma-facing components under the coils such as the divertor plates, and the modular coil case. The CWS shape can be fixed or it can be varied as part of the optimization process, which has the benefit of allowing for further improvement in the physics and engineering objectives. Two methods are used for finding an optimum filamentary coil set on the CWS. The first is to solve for a surface-current distribution on the CWS and then to convert it to a discrete-filament representation. The second is to solve for the filament geometries directly using a parametric representation of their trajectory on the winding surface. The first method uses the NESCOIL code, described briefly in Appendix A (without the discretization of this continuous distribution into coil filaments), and is incorporated in the QPS physics optimization process (as noted above).

The second method for determining coils, a direct-filament method, has been used to design the QPS modular coils. This method uses the COILOPT code, which optimizes the coil geometry on

a toroidal winding surface that is required to be well separated from the plasma boundary. A parametric representation of the filamentary coils is used, with spatial-reflection constraints imposed on the coils to ensure preservation of stellarator symmetry. In addition, parameters in the representation of the winding surface geometry are varied to further improve the optimization targets.

Methods for targeting magnetic surface quality as a coil design objective have been investigated as part of the NCSX project. The most success has been achieved using the PIES code to compute small modifications to the modular coil geometry determined by COILOPT. Coefficients in the modular coil representation are adjusted to cancel the normal magnetic field components at the dominant resonant island chains in the plasma interior. The resulting modified plasma has significantly improved magnetic surface quality (residual islands widths are greatly reduced) in NCSX.

### 4.2. Optimization constraints in coil design using COILOPT.

The COILOPT code solves the stellarator magnetic coil optimization problem by determining the coefficients in an explicit representation of modular coils on a toroidal CWS, together with the coefficients describing the spatial position of the optimal winding surface. Target functions in the optimization problem include the error in the normal component of the magnetic field at the plasma edge (B-normal), the lengths of individual coils, the minimum coil radius of curvature, the minimum separation between adjacent coils and between the coils and the plasma, and the minimum distance across the middle of the torus between opposing coils. These optimization targets are summarized in Table 4.1.

Table 4.1. Optimization targets and figures-of-merit used in the modular coil design process.

| Target | Parameter | Value | Purpose |
|---|---|---|---|
| RMS field error on LCFS (%) | $\delta B_{rms}$ | $\leq 2.0$ | Equilibrium reconstruction |
| Avg. field error on LCFS (%) | $\delta B_{avg}$ | $\leq 1.5$ | Equilibrium reconstruction |
| Max. field error on LCFS (%) | $\delta B_{max}$ | $\leq 10$ | Equilibrium reconstruction |
| Min. coil-coil separation (cm) | $\Delta_{cc,min}$ | $\geq 11$ | Min. coil current density |
| Min. coil-plasma distance (cm) | $\Delta_{cp,min}$ | $\geq 13$ | Access, flexibility |
| Min. radius of curvature (cm) | $\rho_{min}$ | $\geq 7$ | Coil fabrication |
| Coil length (cm) | $L_c$ | $L_0$ | Coil complexity |
| Min. $\lvert y_{coil} \rvert$ (cm) | $y_{min}$ | $\geq 20$ | Access for TF, OH |

The primary goal of the coil optimization is to find a solution satisfying engineering feasibility constraints that will reproduce, or reconstruct, the targeted fixed-boundary equilibrium flux surfaces and plasma properties when the coils and currents are used to create the external

magnetic field in a free-boundary VMEC equilibrium. Free-boundary reconstruction is an important test of the accuracy of the magnetic field approximation problem and is more general than a simple match to the optimized flux surfaces themselves. Indeed, small departures from the targeted flux surfaces are acceptable provided that the physics properties of the free-boundary equilibrium do not degrade those designed into the optimized equilibrium.

### 4.3. Examination of candidate modular coils for QPS

Figure 4.2 shows a top view of a modular coil solution obtained from COILOPT for the reference plasma configuration gb4 (<R> = 1.0m, A = 2.6, $\beta$ = 2%), containing $N_c$ = 8 coils per field period (4 unique coil types). Starting with an approximately conformal 16 cm winding surface with 21 Fourier modes, a sequence of COILOPT solutions targeting minimum coil-coil separation ($\Delta_{cc,min}$), and minimum radius of curvature ($\rho_{min}$), are obtained, while increasing the

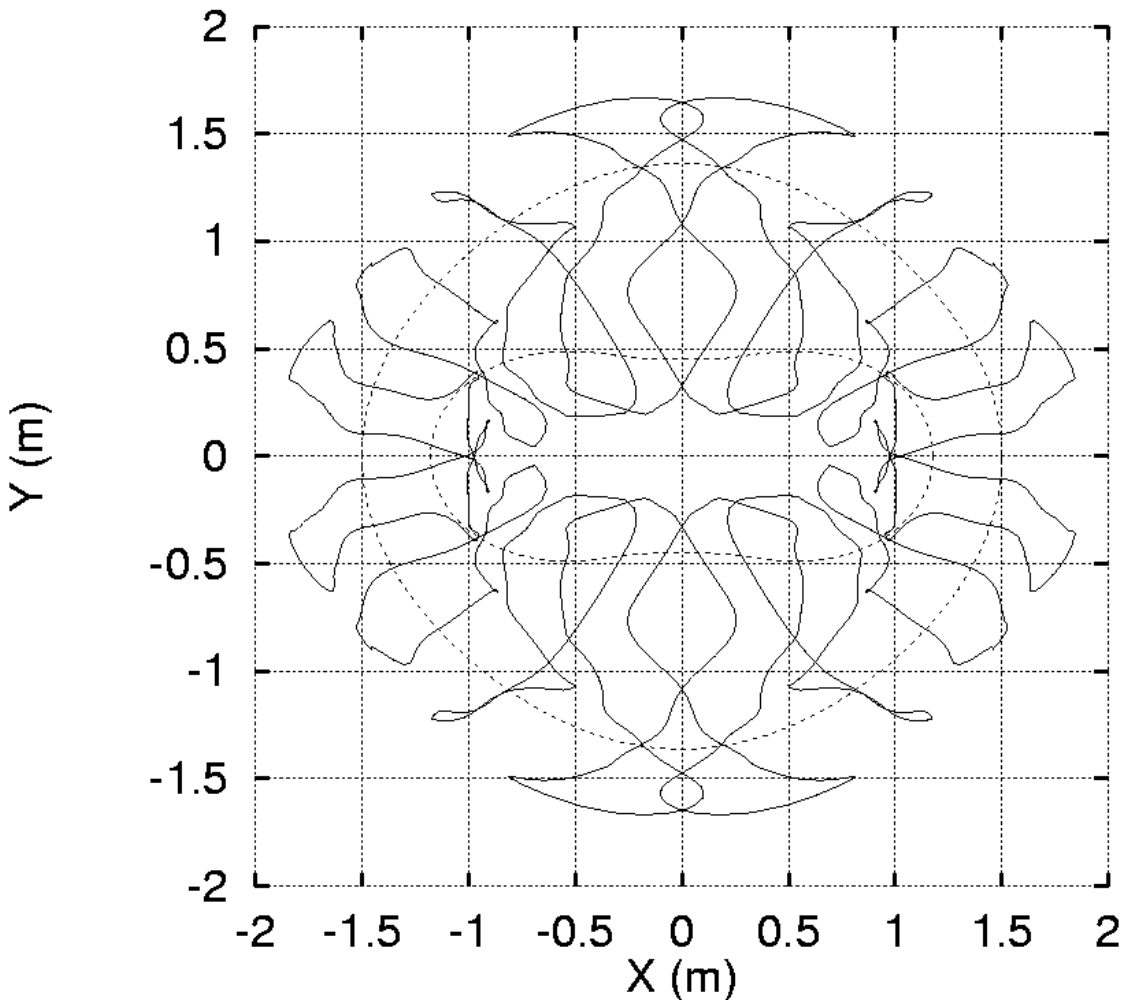


Figure 4.2. Top view of the plasma boundary (dashed line) and filamentary representation of the reference modular coil set 0213b2 (solid line).

surface with 21 Fourier modes, a sequence of COILOPT solutions targeting minimum coil-coil separation ($\Delta_{cc,min}$), and minimum radius of curvature ($\rho_{min}$), are obtained, while increasing the number of modes describing the CWS. The winding surface, containing 41 Fourier modes in the final calculation, is included in the optimization by allowing its coefficients to vary.

For the two field period QPS reference configuration (gb4), optimized modular coils tend to extend into the inboard region of small major radius R, restricting room in the center of the device for TF and OH coils. In order to maintain adequate space on the inboard side of the torus in the optimized coil system, an additional penalty function is imposed on the minimum y-coordinate (see Fig. 4.2) for selected coils near the v = 1/2 toroidal symmetry plane.

Modular coil solutions (with no auxiliary TF or PF coils) with $N_c$ = 8, 10, and 11 coils per field period have been examined for the gb4 plasma configuration, with results summarized in Table 4.2.

Table 4.2. Modular coil optimization results for QPS plasma configuration gb4_nes12a.

| ID | $N_c$ | $\delta B_{avg}$(%) | $\delta B_{max}$(%) | $\Delta_{cc,min}$(cm) | $\rho_{min}$(cm) | $\Delta_{cp,min}$(cm) |
|---|---|---|---|---|---|---|
| 0205b3 | 8 | 3.66 | 29.32 | 9.6 | 6.7 | 11.5 |
| 0206a4 | 8 | 2.06 | 14.95 | 10.0 | 6.7 | 12.0 |
| 0206a10 | 8 | 1.75 | 12.15 | 9.8 | 5.4 | 13.5 |
| 0205a2 | 10 | 2.37 | 15.28 | 8.5 | 5.7 | 12.3 |
| 0129a2 | 11 | 1.86 | 15.64 | 7.7 | 5.3 | 11.2 |

For $N_c$ = 8, modular optimization 0205b3 assumes coils on both symmetry planes (v = 0 and v = 1/2), which implies 5 independent coil types in order to maintain stellarator symmetry. Errors in the match to the normal component of the magnetic field at the plasma boundary for this case are large, and a plasma reconstruction has not been attempted. In contrast, coil system 0206a4, also with $N_c$ = 8, has no coil on either symmetry plane, reducing the number of independent coil types to 4, and gives a much lower field error. Coil sets 0205a2 (with $N_c$ = 10 and no coils on symmetry planes), and 0129a2 (with $N_c$ = 11 and a coil on the v = 1 symmetry plane), both have 5 coil types. The optimizations with 5 coil types typically require constraints on the minimum-y value for 3 coils (per field period, centered at x = 0) to preserve adequate space in the center. Solutions with $N_c$ = 8 and no coils on symmetry planes, however, only require the minimum-y penalty for 2 coils.

The solutions discussed above assume uniform modular coil currents. Optimization 0206a10 is a continuation of 0206a4 with variable coil currents. This solution also includes a pair of axisymmetric VF coils located at R = 1.689m, Z = ±1.0m, with variable coil current. Average field error in this solution is reduced to 1.75% and a free-boundary VMEC equilibrium, using

this modular coil set to create the external field, compares favorably with the fixed-boundary solution from which the target plasma boundary used for this analysis was derived.

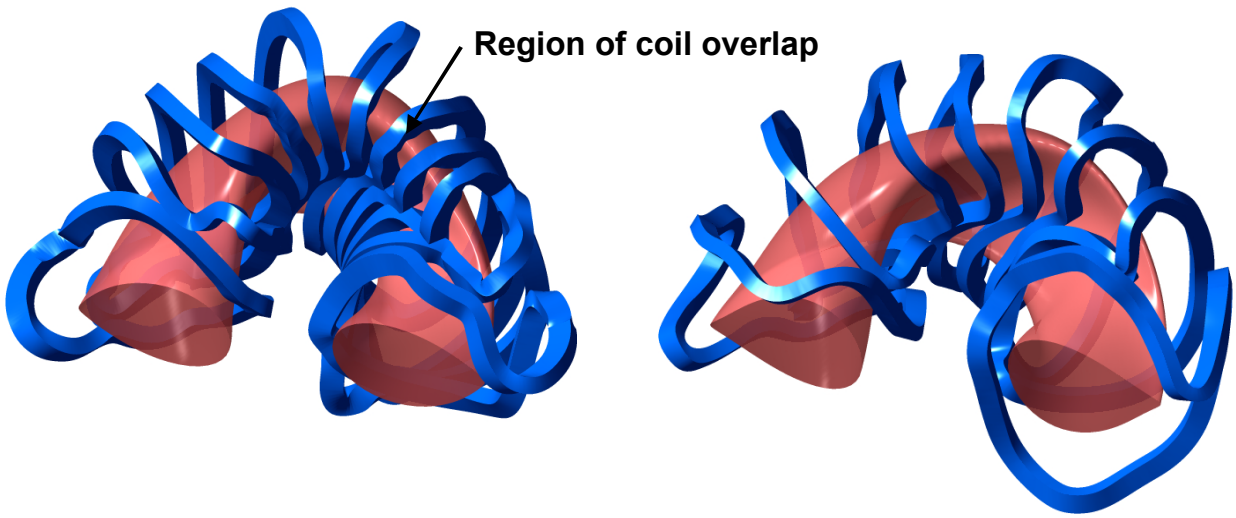


Figure 4.3. Reducing the total number of modular coils from 22 to 16 eliminated the coil overlap problem on the inside corner.

### 4.4. Reference QPS Coil Configuration

Based on the results summarized in Table 4.2, together with a consideration of costs associated with coil fabrication and power supplies, we have concentrated our efforts on improving the properties of a reference coil configuration for the gb4 plasma with:

- eight modular coils per field period
- uniform modular coil currents
- no coils on symmetry planes
- a VF coil with fixed position and variable current.

We find that a significant reduction in field error is obtained, together with improvements in coil geometry parameters, if a relatively small background toroidal field (1/R field), in a direction opposite to that of the modular coils, is included in the optimization. Table 4.3 contains a sample of COILOPT results where the optimization is started from different values of the background toroidal field current (listed relative to the total poloidal current per field period $I_{pol}$) and vertical field coil currents. The VF coil current is varied in the optimization in all cases except 0214a1, where it is set to zero. The 1/R field is either fixed (e.g., 0216a2) or included as a free parameter in the optimization (e.g., 0213b2). Solution 0213b2, chosen as the reference QPS coil configuration for engineering design and analysis, results in an excellent plasma boundary reconstruction, as shown in Figure 4.7.

The symmetry properties of the reference coil set are evident in Figure 4.4, where modular coils are shown in u-v space (u and v are the normalized poloidal and toroidal variables, respectively, used in NESCOIL) for one field period on the final (optimized) winding surface. The reference modular coil design is presented in Figure 4.5.

Table 4.3. Optimization of 8 modular coils per field period, including one pair of vertical field (VF) coils and a toroidal (1/R) field, for QPS plasma configuration gb4_nes12a. Solution 0213b2 is the reference coil configuration.

| ID | $I_{TF}/I_{pol}$ | $I_{mod}$(kA) | $I_{VF}$(kA) | $\delta B_{avg}$(%) | $\delta B_{max}$(%) | $\Delta_{cc,min}$(cm) | $\rho_{min}$(cm) | $\Delta_{cp,min}$(cm) |
|---|---|---|---|---|---|---|---|---|
| 0216a1 | -.071 | 366 | -201 | 1.42 | 9.52 | 11.5 | 7.3 | 13.2 |
| 0213b2 | -.121 | 374 | -205 | 1.43 | 8.66 | 11.4 | 7.2 | 13.4 |
| 0216a2 | -.212 | 391 | -205 | 1.38 | 7.03 | 11.6 | 7.7 | 13.3 |
| 0216a3 | -.283 | 403 | -208 | 1.49 | 7.51 | 11.6 | 6.9 | 13.4 |
| 0216a4 | -.071 | 366 | -90 | 1.64 | 10.22 | 10.4 | 6.6 | 12.5 |
| 0216a5 | -.212 | 391 | -126 | 1.44 | 7.95 | 10.7 | 7.4 | 13.5 |
| 0214a1 | -.107 | 372 | 0 | 2.03 | 11.90 | 8.6 | 6.6 | 12.9 |

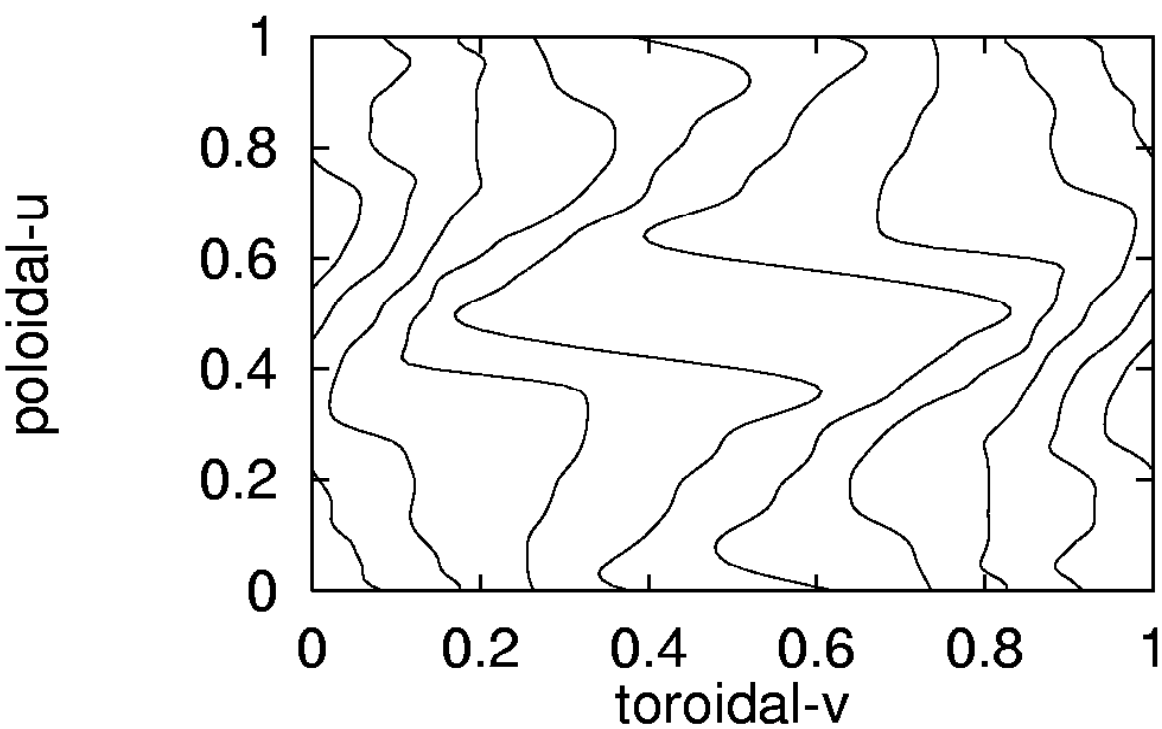


Figure 4.4. Modular coils 0213b2 shown in u-v space for one field period.

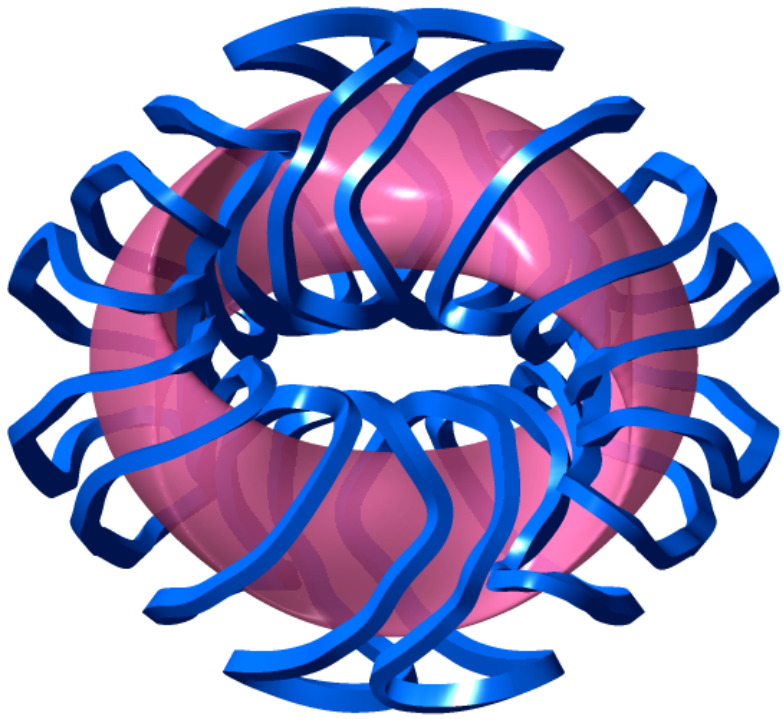

Figure 4.5. The modular coil set 0213b2 for the QPS reference configuration.

### 4.5. VMEC Free Boundary Reconstruction for the QPS Reference Configuration

The modular coil set determined by COILOPT with only eight coils per period has an average field error of 1.43% and a maximum field error of 8.66%. The distribution of these errors in the u-v plane is shown in Figure 4.6. The line of maximum errors follows the path of maximum B on the plasma from v = 0.15, u = 0.4 to v = 0.85, u = 0.6. The significance of this error is determined by how well the free-boundary reconstruction of the equilibrium preserves the physics properties of the original optimized fixed-boundary equilibrium.

The shape of the outer magnetic flux surface is the primary variable that determines the physics characteristics of a stellarator configuration. It is therefore crucial that the QPS coil set determined here reproduce the shape determined by the fixed boundary optimizer as accurately as possible. It is important to verify that the free boundary flux surfaces (produced by the coils) lead to similar physics properties as obtained for the original fixed boundary plasma. Figure 4.7 compares the flux surfaces from the fixed-boundary with the free-boundary calculation based on filamentary coils. The surfaces are quite similar except for the narrow tip regions in the v=1/4 and v=1/2 cross sections.

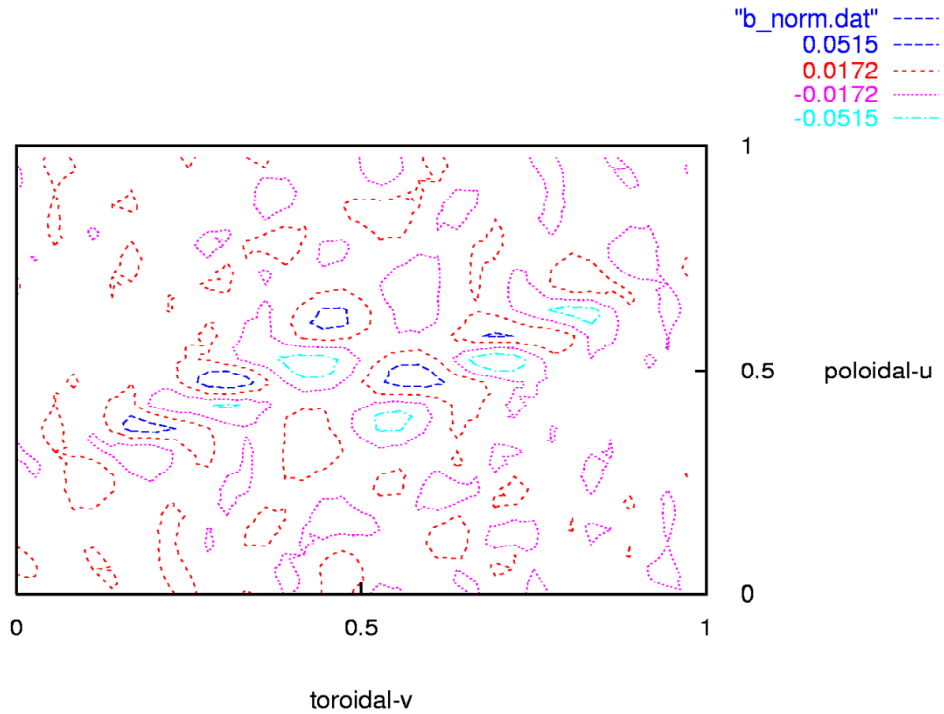


Figure 4.6. Map of $B_{normal}$ errors in the u-v plane for the 0213b2 coil set.

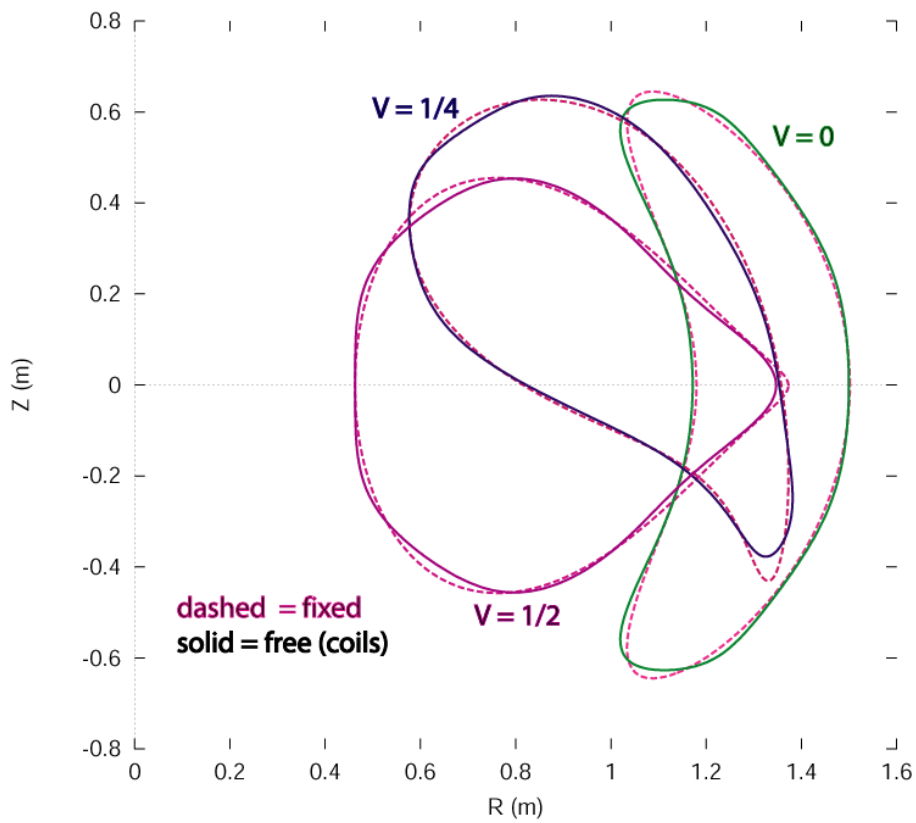


Figure 4.7. Fixed- and free-boundary equilibria are essentially identical for the reference QPS modular coil set 0213b2.

## 4.6. Multi-filament coil model

A single filament was used to represent each modular coil in deriving the reference 0213b2 coil set. The actual cross-section coils shown in Figure 4.5 were obtained from the filamentary coil set subject to engineering constraints on allowable coil clearances, minimum bend radius, twist of the coils, and current density in the coils. A four-filament model (shown in Figure 4.8) was then derived from the finite cross section coils in Figure 4.5 to test the accuracy of the single filament representation for the modular coils. The comparison of the results from the original single-filament coil set and the four-filament model of the coil cross section are shown in Figure 4.9 for the vacuum case and in Figure 4.10 for the $\langle\beta\rangle = 2\%$ case. The crosses in Figure 4.9 indicate where the filaments cross the toroidal plane in Figure 4.8. The single-filament case has a slightly larger LCFS and more rectangularity than the four-filament case in vacuum. A similar behavior is seen in the $\langle\beta\rangle = 2\%$ free-boundary VMEC cases in Figure 4.10. The close similarity of the single-filament and four-filament models gives confidence in our use of the single-filament model for the present level of calculations.

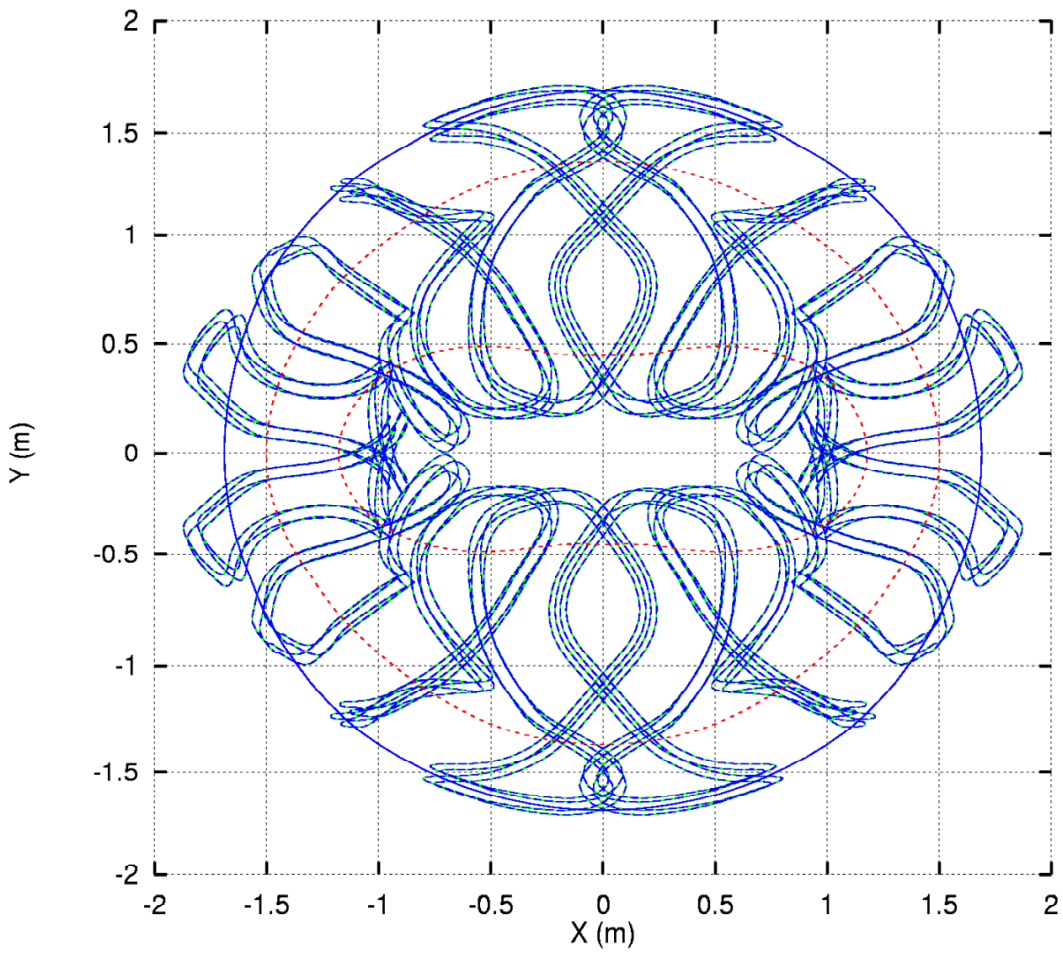


Figure 4.8. Four-filament representation of the QPS reference coil set 0213b2.

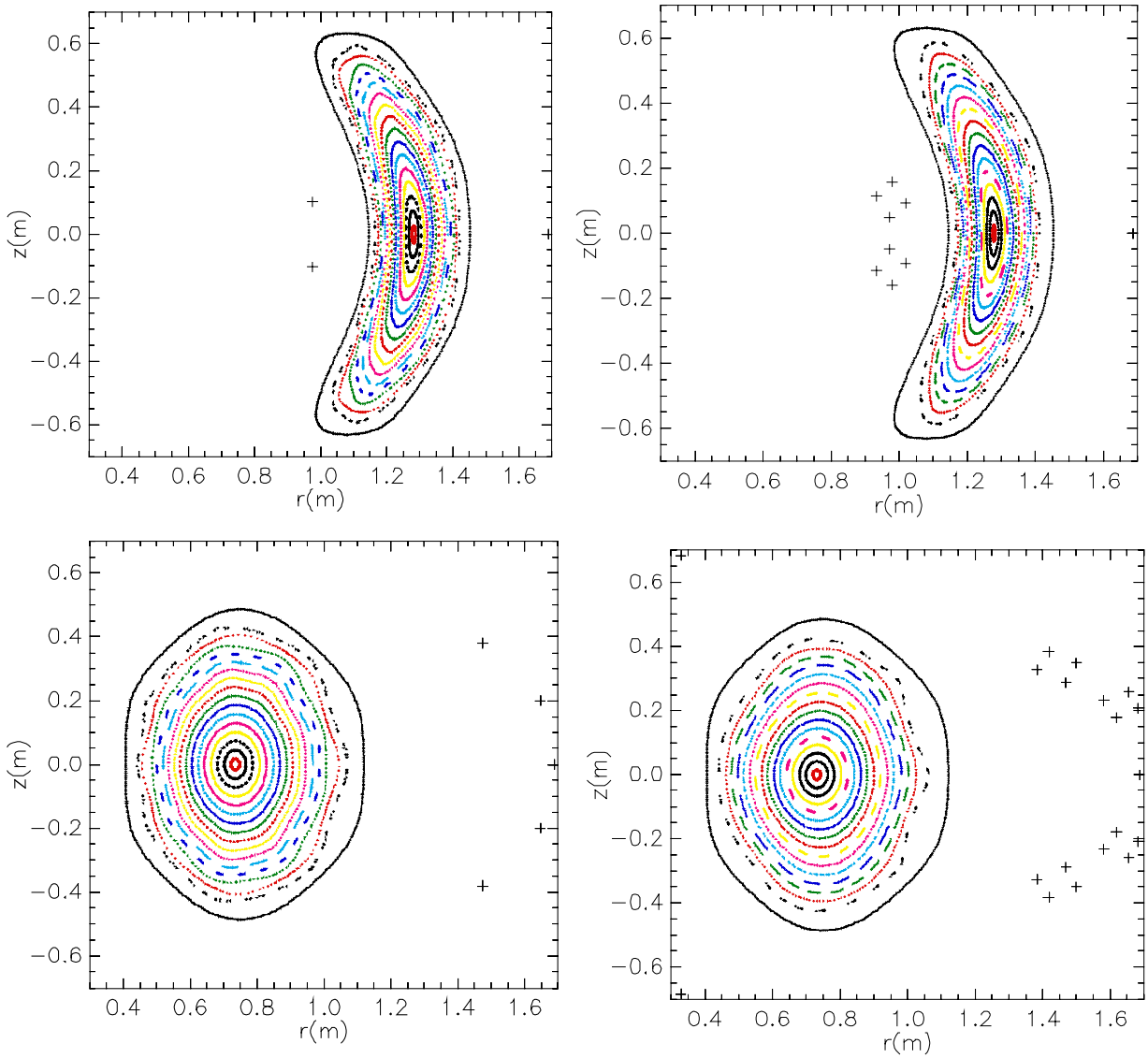


Figure 4.9. Vacuum flux surfaces (in color) from following field lines and the LCFS from the free-boundary VMEC code (in black) at 0º (top row) and 90º (bottom row) toroidally for the single-filament model (left) and the four-filament model (right).

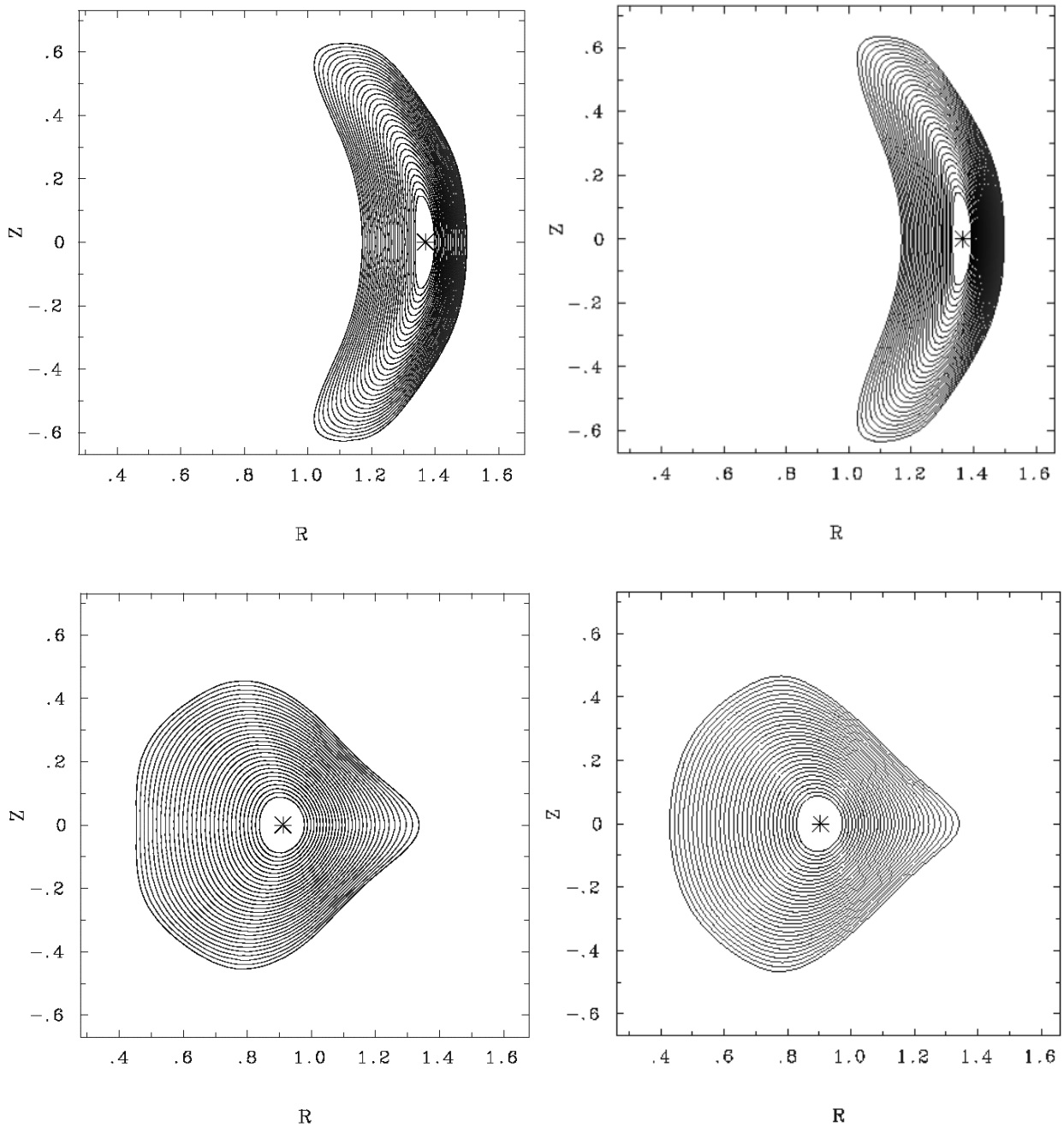


Figure 4.10. Free-boundary VMEC flux surfaces for ⟨β = 2% at 0º (top row) and 90º (bottom row) toroidally for the single-filament model (left) and the four-filament model (right).

## 4.7. Plans to improve the QPS coil configuration

We plan to continue efforts to optimize the QPS modular coils, together with TF and VF coils, to further reduce field errors and coil current density requirements. There is also an effort underway to merge the capabilities of the STELLOPT free-boundary physics optimization with the COILOPT modular coil model in order to use parameters in the current filament representation as independent variables to directly optimize physics properties. Modular coil

solutions developed with the present “reverse-engineering” methods would provide good starting points (initial solutions) for this improved coil design procedure.

### 4.8. Poloidal Field Analysis

The poloidal field coil (PF) set for QPS has three functions: (1) augment the equilibrium coil set (modular and auxiliary TF) in order to adequately reproduce the physics of the reference configuration; (2) vary the plasma configuration with, e.g., vertical and quadrapole fields in order to study particular physics issues; and (3) provide a moderate volt-second capability in order to induce toroidal plasma currents that will assist in plasma startup and configuration variations. The PF coil set includes two pairs of existing axisymmetric coils, the ATF inner- and mid-VF coils, a pair of elliptical coils, and a racetrack-shaped central solenoid. The geometric properties of these coils are illustrated in Figures 4.11 and 4.12.

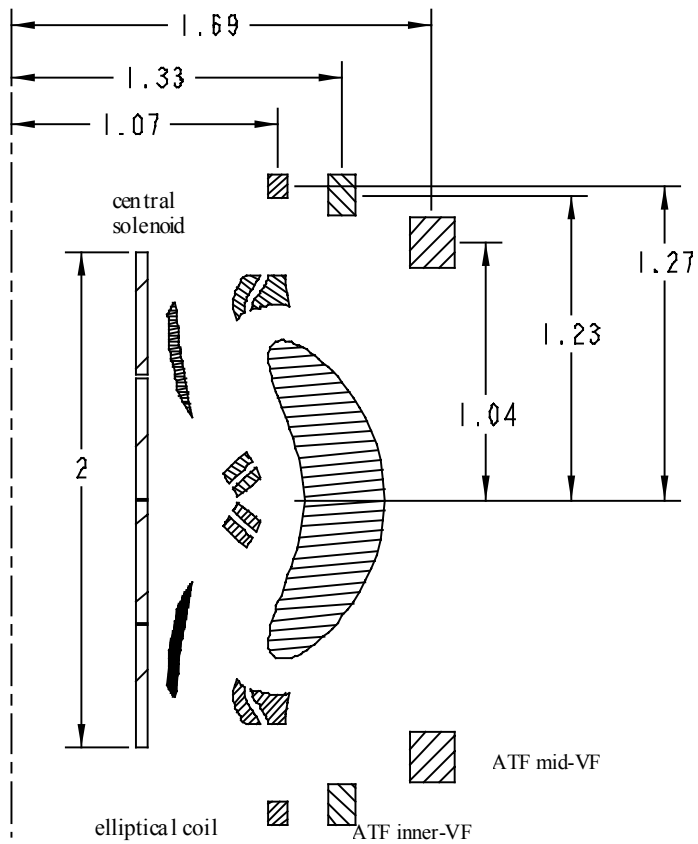


Figure 4.11. Cross section of the QPS poloidal coil set for the "crescent" shaped symmetry plane. This view shows the long dimension of the non-circular coils.

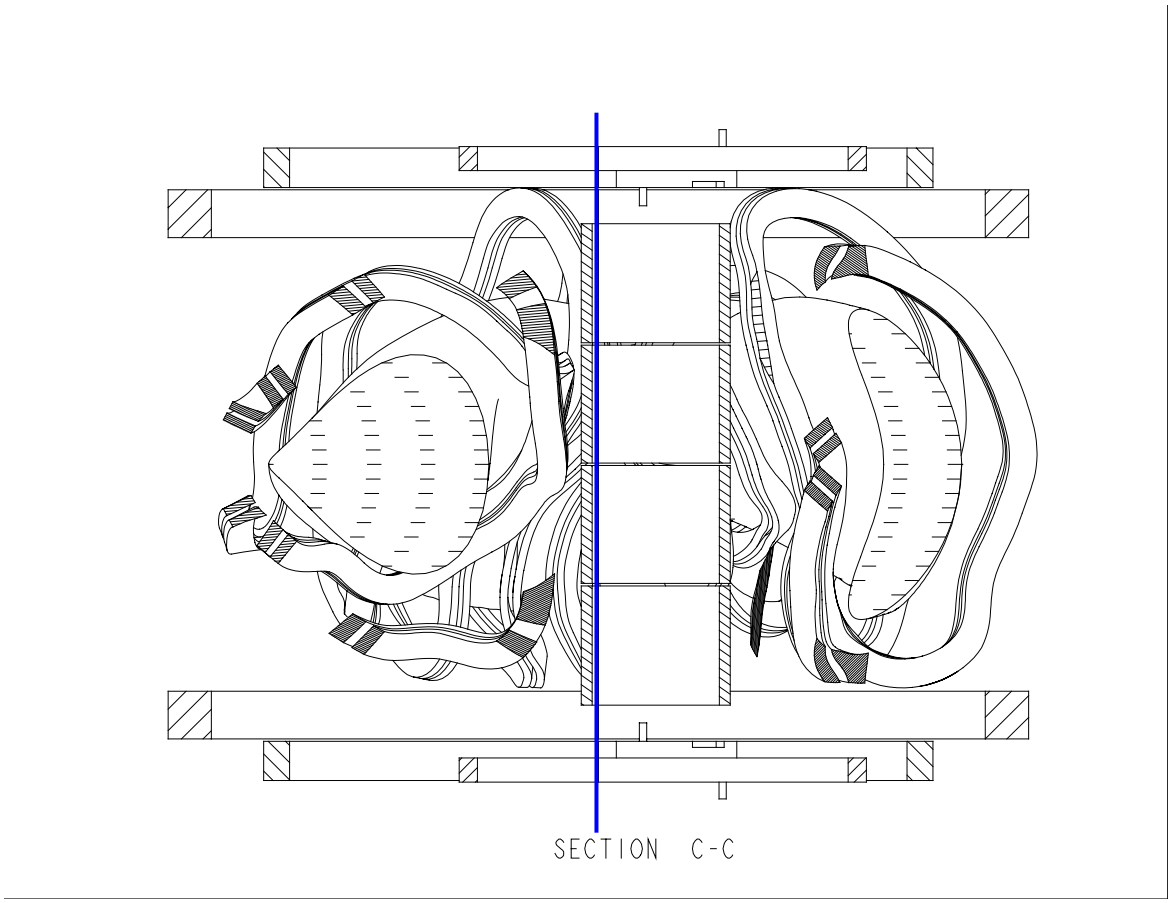


Figure 4.12. Poloidal coil cross sections for both symmetry planes. The non-circular design of the elliptical coil and OH solenoid are seen relative to the blue centerline.

The configuration and flexibility functions of this coil set are presented in Chapter 7. This discussion will focus on the Ohmic heating (OH) function. Volt-second requirements are based on the flux required to establish the desired plasma current (*LI*) and on the pulse length requirements (*Vt*). Estimates of the total plasma inductance, internal plus external, are in the range of 1.0-1.5 μH, depending on the radial current profile. For example, analytical expressions for the external inductance [5] of an axisymmetric torus of the same mean radius and average elongation as the QPS reference configuration give a value for $L_{ext}$ of about 0.72 μH. A flat current profile, $l_i$ = 0.5, contributes an additional 0.32 μH to the total inductance of 1.03 μH. These estimates suggest that a flux of about 0.1 Wb should be adequate to induce OH currents in the range of 50-75 kA.

The plasma resistance is strongly dependent on plasma parameters and is expected to be in the range of 1-10 μΩ. The larger value results from combination of low temperatures, average values less than 100 eV, and moderate Zeffs. Resistive loop voltages are thus expected to be in the range of 0.1 to 1.0 V for typical plasma currents. This suggests that a flux capability of about 0.1 Vs will be needed to sustain 50-75 kA Ohmic currents for times of ~0.1 s. Smaller OH

currents in combination with bootstrap currents could be maintained for times comparable to the 0.5 s modular coil pulse length. Thus about 0.2 Wb should be adequate for most experiments. To meet this need a 2m-high racetrack central solenoid with a flux swing of 0.15 Wb (0.3 when double-swung) is included in the reference design. Ideally, the flux from this solenoid would be excluded from the plasma volume by a set of PF windings. Preliminary analyses for a 4m-high coil indicated that a small current in the mid-VF coil pair, less than 10 kA (about 5% of the 200 kA in these coils used to produce the equilibrium fields) in each coil, will be sufficient to reduce the field errors that result from the OH solenoid from ~0.5%, about 1/3 of the field errors in the modular coil system, to the 0.05% range. At this level, field errors from the OH solenoid should have a minimal impact on plasma properties. Similar compensation for the shorter, 2m solenoid in the reference coil set is anticipated, given the additional flexibility of the elliptical coil and the inner VF coil as well as the ability to split the solenoid into inner and outer pairs. This calculation, however, remains to be done.

The above analysis and the estimate of 0.3 Vs capability did not include the fields and fluxes due to image currents in the aluminum tank. Table 4.4 presents the inductance matrix for the poloidal coils, the straight section of the aluminum vacuum vessel, and the plasma. The non-circular components (central solenoid, elliptical coil, and plasma) are approximated by equivalent area circular systems. Inductances are normalized to their one-turn equivalent values.

Table 4.4. Inductance matrix for the reference QPS poloidal coil System. All values are in micro Henries. Self-inductances on the diagonal are shown in blue. The tank is modeled as a single turn with the same height as the cylindrical portion of the vacuum tank.

| | PF1 | PF2 | PF3 | PF4 | PF5 | Tank | Plasma |
|---|---|---|---|---|---|---|---|
| PF1 inner solenoid | 0.38 | 0.05 | 0.03 | 0.07 | 0.09 | 0.05 | 0.11 |
| PF2 outer solenoid | 0.05 | 0.33 | 0.09 | 0.09 | 0.09 | 0.04 | 0.06 |
| PF3 elliptical | 0.03 | 0.09 | 4.22 | 1.15 | 0.93 | 0.41 | 0.27 |
| PF4 ATF inner | 0.07 | 0.09 | 1.15 | 11.05 | 6.10 | 2.28 | 0.87 |
| PF5 ATF mid | 0.09 | 0.09 | 0.93 | 6.10 | 14.34 | 4.14 | 1.16 |
| Cylindrical tank | 0.05 | 0.04 | 0.41 | 2.28 | 4.14 | 3.18 | 0.68 |
| Plasma | 0.11 | 0.06 | 0.27 | 0.87 | 1.16 | 0.68 | 1.44 |

The tank significantly complicates the poloidal design because its large mutual inductances with other PF coils, as shown in Table 4.4, and its low resistivity. Mutual inductances of the PF coils to the plasma are the 1/4 – 2 times those of the PF coils to the tank. Thus currents induced in the tank by the PF coils (image currents) are the same order as those induced in the plasma. The ~4 μΩ tank resistance combined with the self-inductance of ~3 μH yields an L/R time constant of ~0.75 s. As a result, the magnetic fields that result from driving a current in any one coil will, during this time period, consist of the field due to that coil <u>and</u> the opposing field of its slowly decaying image.

The presence of image fields complicates the design of both the equilibrium coil set discussed earlier in this chapter and of the PF set. The mid-VF coil is used for producing equilibrium fields and its image was not included in the modular coil design optimization. These image fields largely cancel the fields produced by the mid-VF coil itself, and must be included in error analysis and plasma reconstructions. While a new modular coil set could be designed including fields from the image, its time dependence and non-axisymmetric structure due to tank ports pose a significant challenge. The impact on the PF design is also significant. For example, the mid-VF coil is strongly coupled to the tank, and, due to field cancellations by image currents, much larger values of mid-VF current will be needed to cancel error fields from the OH solenoid. Producing these currents on the OH time-scale will increase needed power supply voltages. Calculations to estimate the power supply requirements to produce time variations on the ~0.1 s time scale are planned, but not yet completed.

As a result of the issues discussed in the PF analyses, we are exploring replacing the cylindrical component of the present vacuum vessel with a stainless steel structure. The time constant will be smaller due to the 40-times higher resistivity of stainless compared to aluminum and the potential reduction in thickness by a factor of two to three. These two effects would bring the time constant down to ~10 ms, smaller than typical current and configuration evolution times. The complications due to image currents on this time scale are likely manageable.

## 4.9. Summary

After examining several options for QPS coils, a reference configuration consisting of eight modular coils per field period with uniform currents and no coils on the symmetry planes, and a pair of existing vertical field coils, has been chosen as a reference for engineering studies. The modular coil geometry and VF coil current were combined with a relatively small 1/R field in a COILOPT optimization model to produce a QPS coil system satisfying physics performance properties and engineering design criteria. Free-boundary VMEC reconstruction of plasma properties and an analysis of vacuum flux surface quality show an accurate approximation of the targeted plasma. A preliminary analysis of the QPS poloidal field suggests that a 2-m high central solenoid in combination with the ATF mid-VF coil (also used in the reference equilibrium coil set), the ATF inner-VF coil, and an elliptical coil should provide adequate volt-

seconds of OH currents and sufficient shaping flexibility. The use of a stainless steel replacement for the existing aluminum cylindrical vacuum vessel is appears to be a promising solution to the long time constants of the aluminum component.

## References


[1] Hirshman, S.P., Spong, D.A., Whitson, J.C., et al., *Phys. Plasmas* **6** (May, 1999) 1858.
[2] Spong, D.A., Hirshman, S.P., Whitson, J.C., et al., *Nuclear Fusion* **40** (March, 2000) 563.
[3] Spong, D.A., et al. to be published in *Nuclear Fusion* (2001).
[4] Merkel, P., *Nuclear Fusion* **27** (1987).
[5] Hirshman, S.P. and Neilson, G.H., *Phys. Fluids* 29, 790 (1986).